Methods of Fetal MRI

Peter C. Brugger

Contents

P.C. Brugger
Integrative Morphology Group, Center of Anatomy and Cell Biology, Medical University of Vienna, Waehringerstrasse 13, 1090 Vienna, Austria
e-mail: peter.brugger@meduniwien.ac.at

D. Prayer (ed.), *Fetal MRI*, Medical Radiology,
DOI: 10.1007/174_2010_29, © Springer-Verlag Berlin Heidelberg 2011

Abstract

› Fetal magnetic resonance imaging (MRI) differs in many respects from a postnatal MRI study. The operator has no influence on the position of the fetus, only by proper positioning and repositioning of the surface coil, and/or the pregnant woman, may optimal imaging conditions be achieved. Without using sedation, fetal movements and positional changes make fetal MRI a sort of interactive imaging, with the goal being to acquire a series of continuous, correctly oriented images as quickly as possible. As structures to be imaged are very small, high-quality images are essential for depicting detailed anatomy and pathology. Therefore, a balance between resolution, field of view, slice thickness, and acquisition time must be found. In addition to T2-weighted sequences, several ultrafast sequences are now available that can provide additional information about specific organs or pathologies.

1 Introduction

Since its introduction in the early 1980s, the development of ultrafast sequences and improvements in scanner and coil technology have led to an increased use of fetal MRI (see also Chap. 1). At present, fetal MRI studies are typically performed on a 1.5-T system using phased-array surface coils with 4–8 elements. For experience at higher field strengths, the reader is referred to Chap. 5, and safety issues are discussed in Chap. 6.

2 Differences from Postnatal MRI

Fetal MRI differs in many respects from postnatal MR studies. First, the operator has no influence on fetal position. Second, structures to be imaged are very small and the fetus may be far away from the coil elements. In addition, without sedation, fetal movements may interfere with image acquisition, making fetal MRI a sort of interactive imaging. While there is no influence on the position of the fetus, coil geometry and image quality can be improved by repositioning the coil and/or the pregnant woman. This is of particular importance in larger fetuses and in cases of increased maternal abdominal circumference (Fig. 1).

3 Age-Related Differences

As fetal MRI is usually performed after the 19th gestational week (GW), it covers a time period of more than 20 weeks, in which the fetus grows considerably in size and fetal weight increases by approximately ten times. Apart from the time a given pathology may be detectable, imaging a small fetus is different from imaging a fetus close to term. However, imaging smaller fetuses is an important issue since legal abortion in many countries is only possible before 24 GW.

In young fetuses, imaging is complicated by the small dimensions and the more frequent fetal general movements, and, in advanced stages of pregnancy, the fetus becomes relatively large with respect to the coil. As the

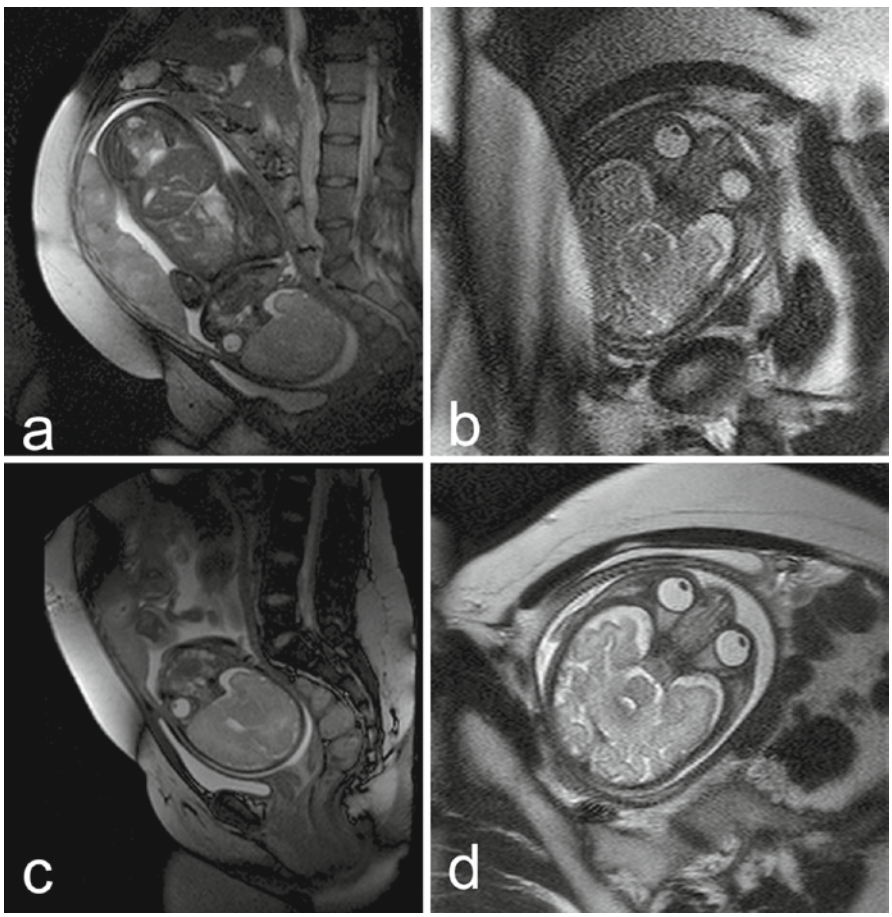

Fig. 1 Repositioning of the coil improves image quality. (**a**) Fetus at 35 + 1 GW. Sagittal image of the initial SSFP survey with center of the coil on the fetal body. (**b**) Low image quality of the resulting axial T2-weighted image through the fetal head. (**c**) SSFP survey with the coil moved more caudally. (**d**) Improved image quality of the axial T2-weighted image through the fetal head

signal-to-noise ratio of the coil decreases toward the edge zones, repositioning of the coil becomes necessary to obtain high-quality images of the fetus. Moreover, the increasing abdominal circumference of the expectant woman also increases the distance between the fetus and the coil elements.

4 Fetal MRI is Whole-Body MRI

Up to 27/28 GW, the relatively small fetal size allows imaging of the whole fetus without repositioning of the coil, although, due to non-alignment of the fetal head with respect to the fetal body, it is usually necessary to image the head and body separately. Assessment of the whole fetal body is particularly important in cases of complex malformations, because diagnosis may only be established by summing up the findings in various organ systems. In addition, extrafetal structures, such as the placenta and umbilical cord, should also be assessed. It is, therefore, advantageous to cover the whole uterus with one sequence to determine the site of umbilical cord insertion.

5 Survey Scan

A steady-state free-precession (SSFP) survey scan yields a total of 42 images in three orthogonal planes of the maternal body in 26 s (Table 1; Fig. 2). It shows the actual position of the fetus and enables a determination about whether the region of interest is within the center of the coil (Figs. 1 and 2). If this is not the case, the coil should be repositioned to guarantee optimal image quality.

The survey scan is more than a simple localizer. Depending on the way the fetus is sectioned, many anatomical details and gross pathologies can be seen on these images. Since the position of the pregnant woman in the scanner is known, as well as the fetuses' position relative to her, the survey scan is also useful for assessing the visceral situs in the fetus. It also provides information on the size and position of the placenta and cervix and the amount of amniotic fluid. Since the scan is planned orthogonal to the body of the pregnant woman, maternal anatomy is also depicted.

6 Planning Sequences and Orientation

Basically, sequences in fetal MRI are planned assuming that the fetus will still be in the same position as on the previous scan. Using the most recent acquisitions in three planes as the basis for the subsequent sequences, the next sequence should be planned immediately after the start of one sequence, so little time elapses between two acquisitions. Although, during the study, there is usually little time to look at the images, one should scroll through the most recent images, look for additional pathologies, and think of sequences that might supply further information.

As the fetus is usually oriented oblique to the standard planes of the pregnant woman, the directions provided by the scanner do not apply to the fetus. Moreover, the orientation of the image plane through the fetus in relation to the pregnant woman also must be taken into account in order to avoid fold-over artifacts. As more or less pronounced changes in fetal position are the rule during the study, appropriate corrections must be made. A keen knowledge of fetal anatomy and spatial imagination are essential in making these corrections.

In planning sequences through the fetal head, the orientation of the axial and frontal planes perpendicular or parallel to the brainstem or the floor of the fourth ventricle is recommended. The interhemispheric fissure and/or the cranial base may be used for proper alignment. These structures can be recognized in smaller fetuses and may be identified even on oblique planes of the survey, or, if fetal motion occurred during the previous acquisition.

Sagittal planes through the fetal head only pose a problem when there is kyphosis of the cranial base. In frontal planes, the superior sagittal sinus can serve as a pointer. Every attempt should be made to acquire an exact median plane, with the tip of the nose, the infundibulum, the aqueduct, and the vermis on one image. An uneven number of slices makes this easier.

Unlike in postnatal whole-body MRI, the long axis of the fetal body is rarely straight, corresponding to the supine position in postnatal imaging. Rather, the long axis usually presents with various degrees of flexion in sagittal and/or frontal planes, or even rotation along its long axis. Consequently, exact orthogonal planes are a compromise. Frontal planes are most useful when there is lateral flexion, as neither strictly orthogonal, sagittal, or axial planes can be planned. Acquisition of exact

Table1 Imaging parameters of sequences used in fetal MRI (1.5 T, Philips, Gyroscan, Best, The Netherlands)

Sequence	FOV (mm)	Matrix	Slice Thickness/ Gap (mm)	TR (ms)	TE (ms)	Acquired Voxel Size (mm)	Reconstructed Voxel Size (mm)	Flip Angle (degree)	Number of Slices	Acquisition Time (s)	NSA
SSFP Survey	400	224×209	7.0	3.13	1.56	1.79/1.79/7.00	1.56/1.57/7.0	60	42	26.2	1
T2 SSH TSE	200	256×153	4.0/0.4 4.0/−1.0	∞	140	0.78/1.18 /4.00	0.78/0.78/4.0	90	18	16.0	1
T2 SSH TSE	230	256×153	4.0/0.4 4.0/−1.0	∞	140	0.90/1.36/4.00	0.90/0.90/4.0	90	18	16.0	1
T2 SSH TSE	200	256×153	4.0/0.4 4.0/−1.0	∞	100	0.78/1.18 /4.00	0.78/0.78/4.0	90	18	13.5	1
T2 SSH TSE	300	256×153	4.0/0.4.0	∞	100	1.17/1.78/4.00	1.17/1.17/4.0	90	18	13.5	1
T2 SSH TSE	275	320×255	4.0/0.4.0	∞	250	0.86/1.08/4.00	0.54/0.54/4.0	90	17	13.5	1
T2 SSH TSE	345	256×148	4.0/0.4.0	∞	80	1.35/2.11/4.00	1.35/1.35/4.00	90	25	21.0	1
SSH MRCP	260	256×205	40–50	8000	800	0.98/1.22/40.0	0.98/0.98/40.0	90	1	<1	1
T1 FFE	325	208×165	5.0/0.5 4.0/0.0	∞	4.6	1.27/1.96/5.00	1.27/1.27/5.0	80	15	15.6	1
SSFP	260	192×219	6.0/−3.0 5.0/−2.5	∞	∞	1.35/1.19/6.00	1.02/1.02/6.0	80	25	20.9	1
SSFP	300	192×255	6.0/−3.0 5.0/−2.5	∞	∞	1.56/1.17/6.00	1.17/1.17/6.0	90	20	21.9	1
SSFP dynamic	320	176×110	7–50	∞	∞	1.82/2.31/7–50.0	1.25/1.25/30.0	60	200	33.6	1
FLAIR	240	192×68	4.0/0.4.0	7000	140	1.35/3.82/4.00	1.02/1.02/4.00	90	18	21.0	2
SSH GRE EPI	230	160×95	4.0	3000	53	1.44/2.42/4.00	0.90/0.90/4.0	90	19	12.0	2
DWI ($b=700$)	250	128×81	5.0	1470	125	1.95/2.31/5.00	0.98/0.98/5.0	90	16	20.1	1
DTI ($b=1{,}000$)	230	112×67	5.0	1649	90	2.05/2.66/5.00	1.80/1.81/5.0	90	12	113	2

FOV field of view; *TR* relaxation time; *TE* echo time; *ms* milliseconds; *NSA* number of signals acquired; *SSFP* steady-state free-precession

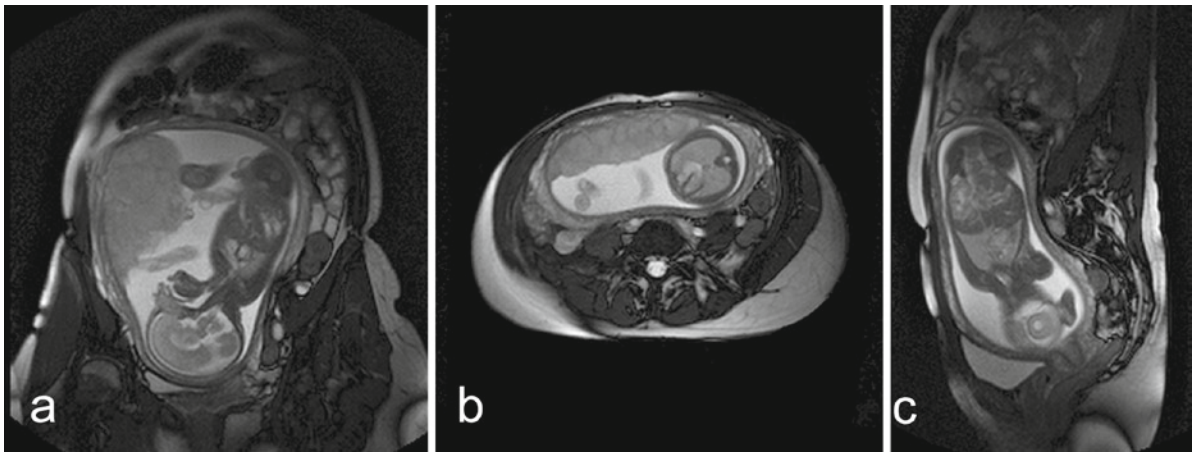

Fig. 2 Selected images of an SSFP survey scan of a fetus at 26+4 GW. (**a**) Frontal image through the pregnant woman provides a sagittal section through the fetal head and allows assessing the male external genitalia. (**b**) Axial image showing the anterior positioned placenta also yields an axial slice through the fetal thorax, depicting the heart and lungs. (**c**) Sagittal image showing the position of the cervix

sagittal planes may also be complicated when the trunk has an oblique elliptical cross section. This frequently happens in cases where there is little amniotic fluid, as when the fetal body is squeezed between the uterine walls and/or placenta. Moreover, in most fetal positions, sagittal images will also include the fetal extremities. Although neither sagittal nor frontal planes will be exactly orthogonal in many cases, fewer images are needed compared to axial planes. Acquisition of axial images through the whole fetal body results in longer acquisition times, as more images are required. This is especially true in larger fetuses in which acquisition of an axial stack may last longer than 1 min.

In case of pronounced flexion of the fetus (curl up position), the fetal thorax and abdomen may have to be imaged separately to obtain axial images, or the acquisition of a radial stack may be indicated.

In general, it is helpful to plan different sequences in the same plane to facilitate comparison of signal intensities of organs or lesions (Fig. 6).

7 Movements

7.1 Fetal Movements

Without sedation, fetal movements will occur during a fetal MRI study. The different patterns of fetal movements and their changes with gestational age are discussed in Chap. 13. As fetal activity is subject to a circadian rhythm (Ehrström 1984), the time when MR is performed might have an impact on imaging. However, while more than half the fetal MRI studies at our institution are made between 7 and 8 o'clock in the morning—a time when a minor peak in fetal activity is reported (Ehrström 1984)—fetal movements are only rarely a problem. Although no constant pattern can be recognized when fetal movements occur during a study, they tend to be rare at the beginning of the study. As imaging focuses on the fetal head or trunk in most cases, the more frequent extremity movements are less of a problem.

Episodes of fetal movements usually last for several minutes, while continuous fetal bulk motion is the exception. Usually, it is possible to continue imaging by repeating sequences in the most amenable plane (e.g., perpendicular to the rotational axis). In doing so, several sequences may be necessary to obtain the desired section plane. In case of persistent fetal bulk motion, dynamic SSFP sequences enable the monitoring of fetal movements and determining when they stop. As a last resort, a new survey scan may become necessary.

In general, fetal movements will depend on gestational age and the space available, and thus, will be more pronounced in younger fetuses and in cases of polyhydramnios. While oligohydramnios restricts fetal movements, the impact of maternal breathing movements on positional changes of the fetus increases, as excursions of the diaphragm or the anterior abdominal wall are directly translated onto the fetus.

7.2 Maternal Breathing Movements

The effect of maternal breathing movements is best demonstrated either by using dynamic sequences or by reformatting a stack of images (Fig. 3). Their impact on dislocation of the fetus depends on fetal position and the amount of amniotic fluid present. Furthermore, in larger fetuses, it is more likely that the fetus is in contact with the uterus, the placenta, or the anterior abdominal wall. Abdominal breathing leads to an anterior–posterior dislocation of the fetus being more pronounced in the cranial half of the uterus, while diaphragmatic breathing movements cause a cranio-caudal shifting. To prevent breathing movements that affect the accuracy of volumetry, sequences acquired for volumetrical purposes should be performed during maternal breath-hold.

7.2.1 Image Acquisition During Maternal Breath-Hold

With regard to maternal breathing movements, fetal MRI faces problems similar to abdominal MRI. In our experience, image acquisition in maternal breath-hold is primarily indicated when using T1-weighted sequences, which are performed in a single breath-hold lasting for 16 s. Other situations in which maternal breath-hold is advisable include oligohydramnios, when the region of interest is subject to maternal breathing movements, especially when volumetry should be performed.

8 Resolution

Dealing with small structures makes resolution an important issue in fetal MRI, as visualization of anatomical and pathological detail depends, in large part, on the spatial resolution of the images and the dimensions of the structure under consideration.

8.1 In-Plane Resolution: Less is More

At least on 1.5-T magnets, the optimal pixel size appears to be on the order of 0.7–0.8 mm. Figure 4 demonstrates that a higher acquisition matrix does not

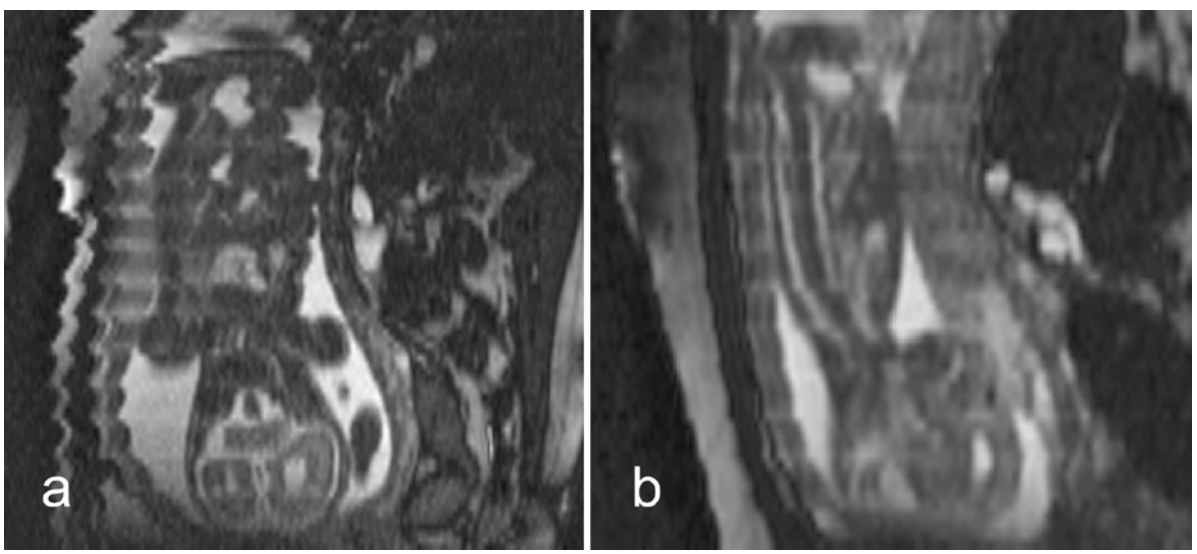

Fig. 3 Visualization of maternal breathing in fetuses with a cephalic presentation. (**a**) Fetus at 27 GW. Reformatted image from an axial stack of 84 SSFP images demonstrates maternal breathing movements during the acquisition: the outline of the pregnant woman's ventral abdominal wall looks like a saw-blade. Note that the effect of breathing on the fetus is most pronounced where the fetal body is in contact with the maternal abdominal wall. (**b**) Reformatted image from an axial stack of 55 SSFP images (2.5 mm distance between slices) in a fetus at 17 + 3 GW. No maternal breathing is evident. The reformatted image allows identification of the fetal spinal canal and aorta

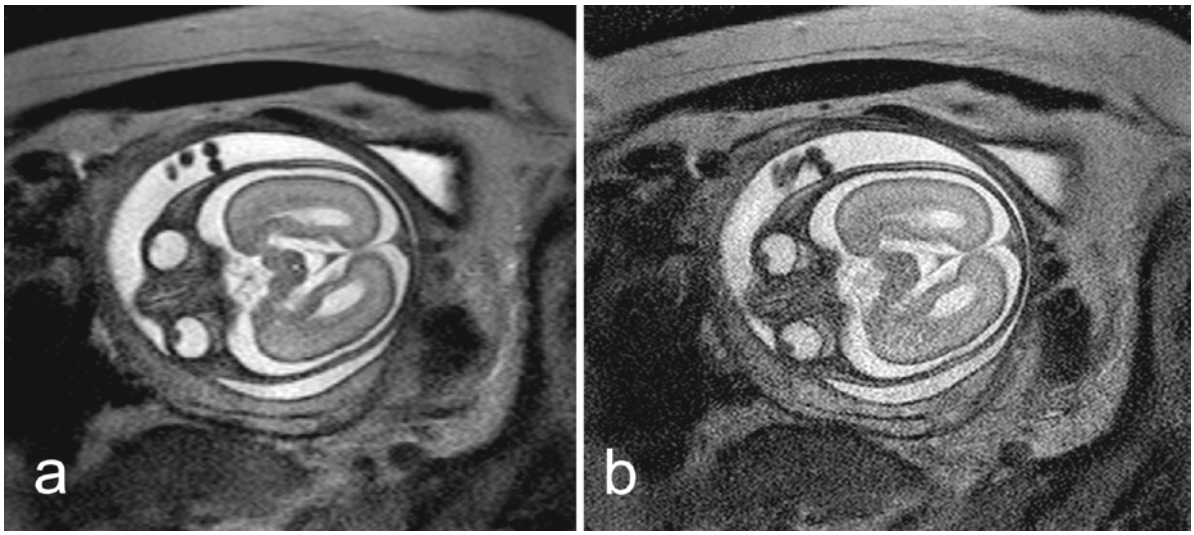

Fig. 4 In-plane resolution and image quality: Corresponding axial T2-weighted images (FOV 200 mm, slice thickness 4.0 mm, gap 0.4 mm) through the head of GW 25+0 fetus. (**a**) Acquired voxel size 0.78×1.18 mm, reconstructed voxel size 0.78 mm. Acquisition time for 18 images was 16 s. (**b**) Acquired voxel size 0.6×0.7 mm, reconstructed voxel size 0.48 mm. Acquisition time for 18 images increased to 22.4 s. Note that neither the optic structures nor the internal carotids and the patent aqueduct can be neatly discerned on the "higher resolution" image

lead to better image quality, but results in more grainy images that veil anatomical detail. While voxel size should be adapted to the size of the fetus or the organ in question, the FOV should be adjusted to maternal body habitus to avoid fold-over artifacts (Fig. 5). However, the larger FOV increases acquisition time, and therefore, the likelihood of fetal motion occurring during the acquisition.

8.2 Slice Thickness

Minimum slice thickness is limited by an increased signal-to-noise ratio. While a 4 mm slice thickness is usually sufficient in larger fetuses, thinner slices are appropriate in smaller fetuses. Using over continuous slices in fetuses less than 25 GW, T2-weighted sequences may be acquired with a distance between

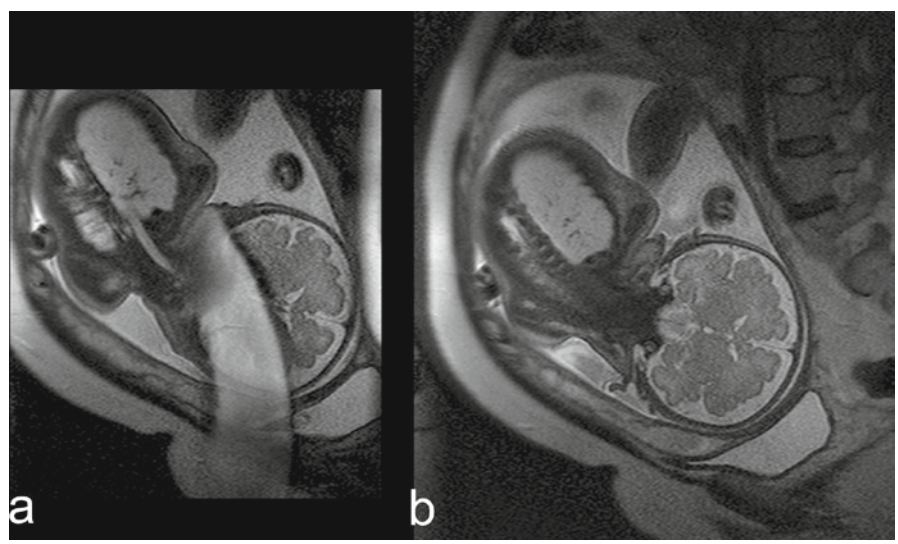

Fig. 5 Frontal T2-weighted images through the fetal head (35+4 GW). (**a**) Typical fold-over artifact using a FOV of 230 mm (stack of 32 images acquired in 23 s). (**b**) Same sequence and resolution: The larger FOV (300 mm) eliminates the artifact, but increases acquisition time to 32 s

slices of 3 mm, and SSFP sequences with a distance of 2.5 mm. T1-weighted sequences may be acquired with a 4 mm slice thickness without gap.

9 Sequences

To date, many so-called ultrafast sequences are available in fetal MRI (Fig. 6). Typically, the acquisition of 18–25 images takes 14–22 s. Sequence parameters will depend on the type of scanner used; those set forth in Table 1 are based on the author's experience with a 1.5 T Gyroscan (Philips, Best, The Netherlands).

9.1 T2-Weighted Sequences

High-resolution T2-weighted TSE sequences (Table 1) are the mainstay in prenatal MRI to depict normal and pathologic fetal anatomy. Provided there is sufficient contrast and using the right section plane structures, a size of 1.5–2 mm can be depicted (Fig. 7). The presence of amniotic fluid around the fetus provides a perfect contrast to the fetal surface. As most fetal body cavities are also fluid-filled, the nasal and oral cavities and the middle and inner ear can be demonstrated. The fetal stomach and, with advancing gestation, the intestines, are fluid-filled (Fig. 6). The same holds true for the trachea, gallbladder, the renal pelvis, and the urinary bladder.

The physiologically wide external cerebrospinal fluid spaces allow delineation of the cerebral surface and developing gyration (Fig. 7).

The T2-weighted signal intensity of the fetal lungs increases with advancing gestation and is used to assess fetal lung maturation (c.f. Chap. 16).

Vessels surrounded by fluid (extracorporeal umbilical vessels, intracranial arteries, veins, and sinuses) or hyperintense tissues (lung vessels in later stages of gestation) can be depicted using T2-weighted TSE sequences.

T2-weighted imaging with longer echo times enhances contrast and is helpful in demonstrating the intrinsic structure of cystic lesions (e.g., congenital cystic adenomatoid malformations of the lungs).

As a matter of fact, assessment of the fetal surface is limited in cases of pronounced oligohydramnios, while this does not impair visualization of the internal details.

9.2 Thick-Slab Imaging

MR fetography was introduced by Terakoshi et al. (2000) as an alternative to single-shot, fast spin echo MR imaging. While these authors used maximum intensity projections of heavily T2-weighted sequences, today thick-slab acquisitions with a slice thickness of 30–50 mm are used to image the fetus (Table 1; Fig. 8a). Images obtained in this way provide a three-dimensional impression of the fetus and its surroundings. In planning this sequence, intrauterine geometry

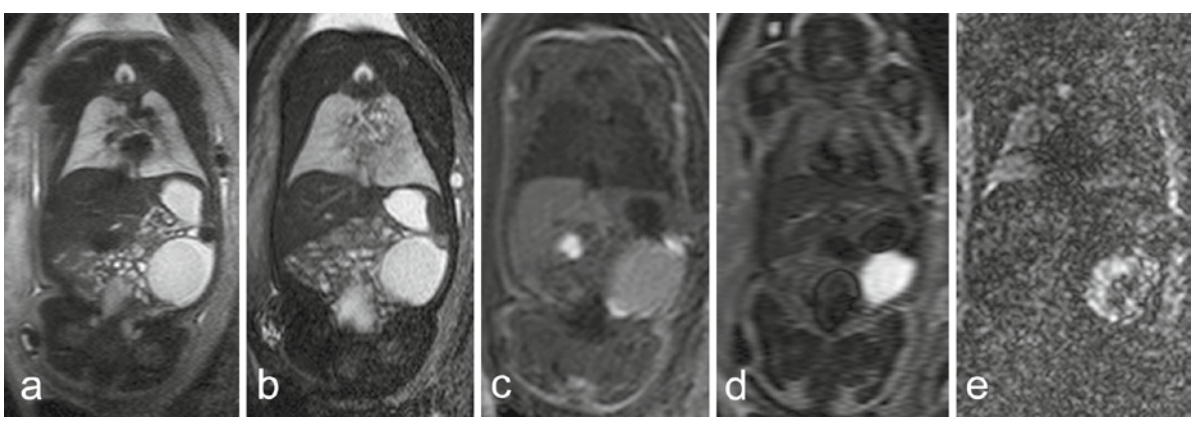

Fig. 6 Corresponding frontal images of different sequences from a female fetus at 36+4 GW with a left-sided ovarian cyst. (**a**) T2-weighted image. (**b**) SSFP image. (**c**) T1-weighted image. (**d**) FLAIR image. (**e**) Diffusion-weighted isotropic image. The hemorrhagic nature of the cystic content is most conspicuous on the FLAIR image

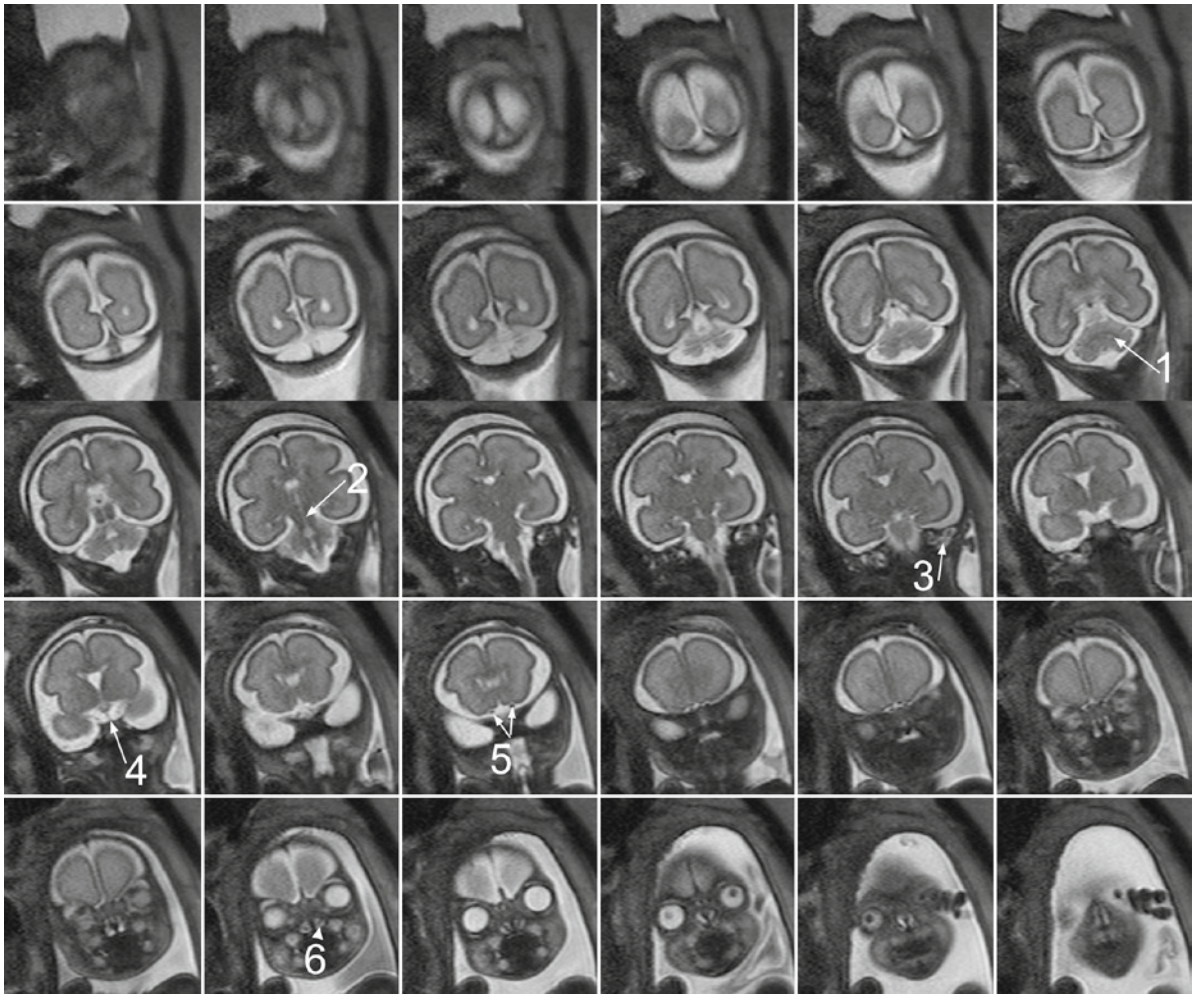

Fig. 7 Set of continuous T2-weighted images (distance between slices, 3 mm) through the fetal head at 26+6 GW. Anatomical details, such as the dentate nuclei (*1*), aqueduct (*2*), ear ossicles (*3*), infundibulum (*4*), olfactory tracts (*5*), and inferior nasal conchae (*6*), can be recognized

must be taken into account in order to avoid projection of the uterine wall or placenta into the image. Maximum slice thickness is, therefore, limited by intrauterine geometry. Another limitation is that at least some amniotic fluid has to be present.

Transparency is increased by shorter echo times, or, alternatively, by using SSFP sequences, which can also be acquired in the thick-slab mode (Fig. 8b). The spatial impression is increased when several images are planned as a radial stack along the long axis of the fetus. With regard to radial acquisition, SSFP sequences are faster, as they have a much shorter preparation phase.

While, in a given case, much information can be drawn from thick-slab images, they cannot substitute for "normal" sequences, which are still necessary for further evaluation. However, this kind of imaging is especially helpful to parents and those who are not familiar with sectional anatomy.

9.3 Steady-State Free-Precession Sequences

While principally providing information similar to that of T2-TSE sequences, steady-state free-precession (SSFP) sequences (Table 1) have the advantage

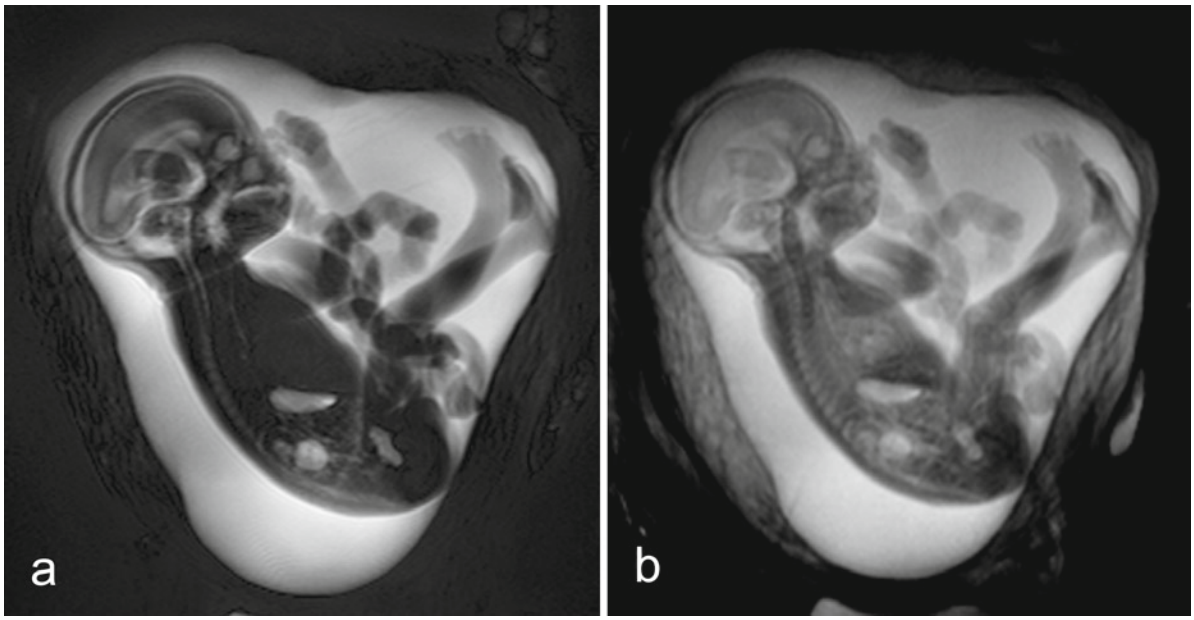

Fig. 8 Sagittal thick-slab acquisitions (40 mm slice thickness) of a fetus at 23 + 1 GW with moderate hydronephrosis. (**a**) T2-weighted image (TE 800 ms). (**b**) Corresponding SSFP image, which is more translucent

that images are immediately reconstructed during acquisition, thus providing "online" information. This makes it easier to determine the latest fetal position in case the fetus moved during the acquisition. SSFP sequences are superior to T2-TSE sequences in visualizing vessels, especially when these are surrounded by dense tissues (e.g., hepatic veins, neck vessels) (Figs. 2 and 9). To date, they are the only sequences to demonstrate fetal cardiac anatomy in greater detail (c.f. Chap. 18).

9.4 T1-Weighted Sequences

Fast low angle shot (FLASH) sequences benefit from acquisition during maternal breath-hold. Parallel imaging allows the acquisition of 15 images in less than 16 s, but makes these sequences prone to artifacts. Usually, 15 images (5.0/0.5 mm slice thickness/gap) are sufficient to cover the whole fetal body in a frontal plane (Table 1). As fewer slices are needed in younger fetuses (<24 GW), slice thickness may be reduced to 4 mm (without gap), increasing the resolution along the *z*-axis at the same time.

T1-weighted sequences allow selectively the demonstration of the fetal pituitary, thyroid (Chap. 19), and liver. These sequences are vital in fetal abdominal imaging, as meconium within the bowels is characterized by T1-weighted hyperintensity (Fig. 10; Chap. 27). Fat suppression is usually not necessary, since adipose tissues develop only with advancing gestation. However, fetal lipomas, such as corpus callosum lipomas (Kim et al. 2002), can be identified in the third trimester. Ossified parts of the skeleton are hypointense and become more clearly visible closer to term (Fig. 11c). Moreover, hemorrhage and even diluted blood (Verswijvel et al. 2002) can be demonstrated using T1-weighted sequences.

9.5 Echoplanar Imaging

Echoplanar sequences (Table 1) allow a rather selective visualization of the fetal skeleton: bones appear hypointense while the cartilaginous parts of the skeleton are hyperintense (Fig. 11). However, with advancing gestation, the contrast between fetal long bones and the surrounding muscles becomes less pronounced. While most organs present with intermediate signal intensity,

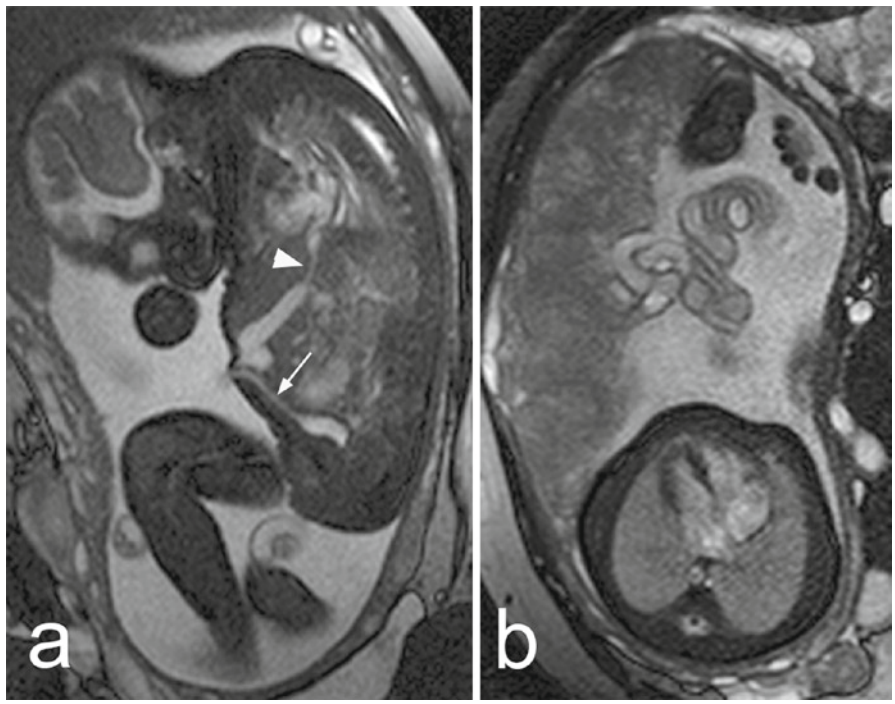

Fig. 9 (**a**) Sagittal SSFP image (fetus at 31 GW) shows the intraabdominal portion of the umbilical vein, its continuity with the ductus venosus (*arrowhead*), and the hepatic vein draining into the right atrium; umbilical artery (*small arrow*). (**b**) Axial SSFP image (2.5 mm distance between slices) through the thorax of a fetus at 30 + 4 GW shows the heart, aorta, and azygos vein, as well as the umbilical cord insertion

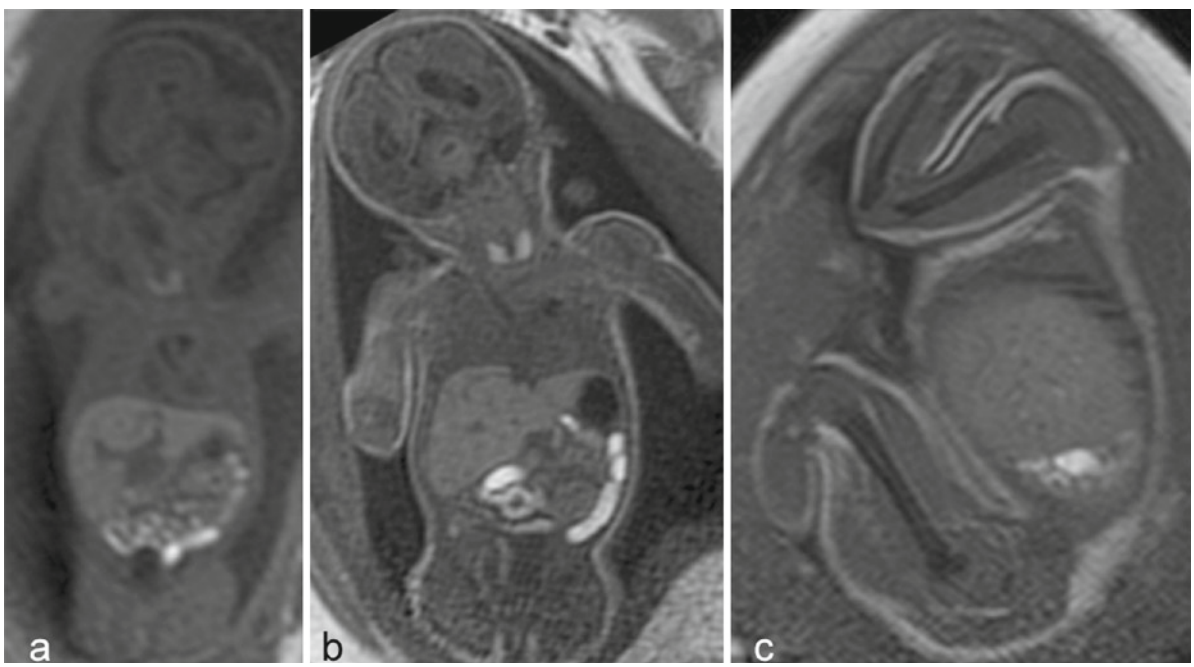

Fig. 10 T1-weighted images. (**a**) Frontal image of a fetus at 22 + 0 GW. (**b**) Fetus at 31 + 0 GW. The liver and thyroid display hyperintense signal intensity, and meconium within the fetal bowels shows marked T1-weighted hyperintensity. The subcutaneous fat layer is evident in (**b**). (**c**) Sagittal T1-weighted image of a fetus at 37 + 3 GW shows well-developed subcutaneous adipose tissues, and the fetal long bones are distinguished by their marked hypointense signal from the muscles, showing intermediate signal intensity

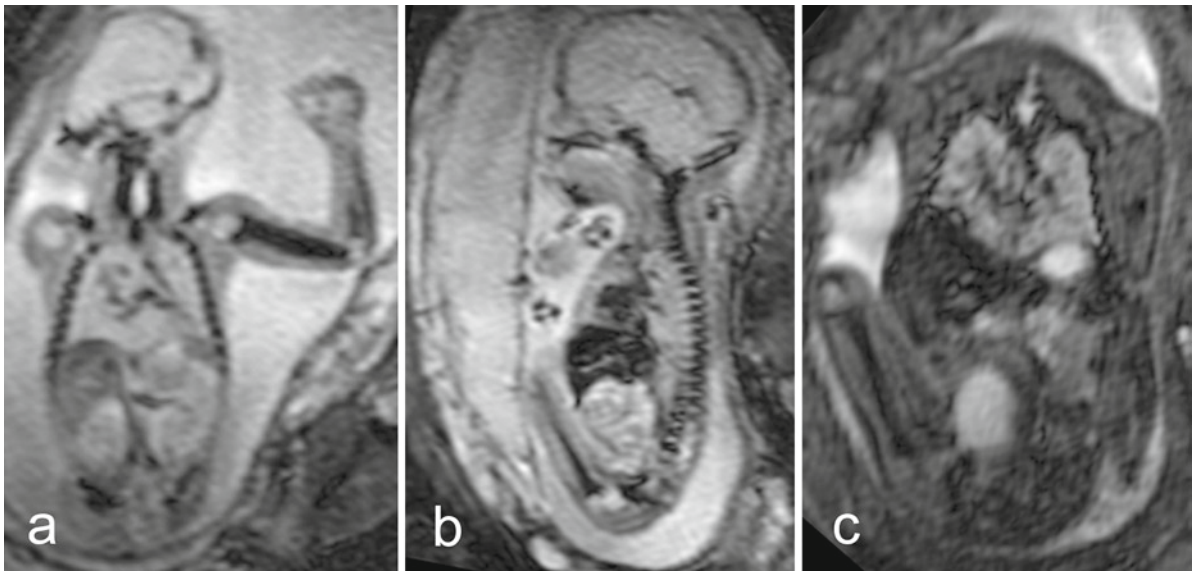

Fig. 11 Echoplanar images. (**a**) Frontal image in a 22+0 GW fetus. (**b**) Sagittal image in a 22+5 GW fetus. The hypointense-appearing fetal bones contrast well against the surrounding structures, and the cartilaginous parts of the skeleton are hyperintense. (**c**) Frontal image in a 31+5 GW fetus demonstrates the decreasing contrast between bone and muscle

the fetal liver usually has hypointense signal characteristics. Furthermore, flow void makes vessels and the heart appear hypointense. The normal placenta usually displays intermediate to hyperintense signal intensity, which decreases with advancing gestation. Echoplanar sequences are also instrumental in demonstrating blood breakdown products, especially when these no longer present as T1-weighted hyperintense lesions.

9.6 Diffusion-Weighted Imaging

Diffusion-weighted sequences are acquired with a *b*-value of 700 and with three phase-encoding directions (Table 1). Figure 12 shows the effect of different b values on imaging in the fetal brain. With regard to the image quality of diffusion-weighted sequences, it is important that the region of interest is in the center of the coil, especially in larger fetuses. With diffusion-weighted imaging (DWI), fiber tracts of the fetal brain, the kidneys, and teeth buds can be selectively demonstrated. For reasons yet to be determined, the whole fetus (except for the liver) displays diffusion-weighted hyperintensity in the earlier stages of gestation (up to 21/22 GW).

Moreover, it is possible to demonstrate ischemic lesions of the white matter with DWI (Baldoli et al. 2002; Guimiot et al. 2008). DWI has also been used to assess the normal and abnormal developing kidneys

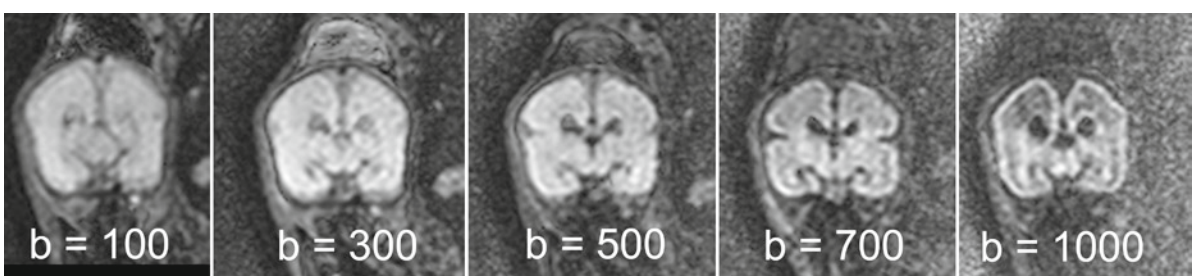

Fig. 12 Corresponding frontal diffusion-weighted images through the head of a fetus at 27+1 GW. With increasing *b*-value, the internal organization of the brain parenchyma becomes evident

(Witzani et al. 2006; Chaumoitre et al. 2007; Savelli et al. 2007). Recently, diffusion tensor imaging using 32 non-collinear diffusion gradient encoding directions has also been applied in utero (Kasprian et al. 2008) (c.f. Chap. 11), allowing demonstration of major fiber tracts of the fetal brain in utero.

9.7 Dynamic Sequences

When there are pronounced fetal movements, the acquisition time of ultrafast sequences is too long and dynamic sequences are the only way to monitor the fetus. We acquire dynamic SSFP sequences with six frames per seconds (fps) and an in-plane resolution of 1.82×2.31 mm, with slice thickness ranging from 8 to 50 mm, depending on the issue at hand (Table 1). As in other thick-slab acquisitions, the maximum slice thickness is limited by the intrauterine space available. With 6 fps, the temporal resolution is high enough to be called real time, as the animated images result in a movie as long as the original acquisition time and show smooth fetal movements. Apart from capturing fetal general movements, dynamic scans are useful in demonstrating intrinsic fetal movements, such as swallowing (Fig. 13), bowel peristalsis, breathing movements, and the beating heart (c.f. Chap. 18).

9.8 FLAIR Sequence

Fluid-attenuated inversion recovery (FLAIR) sequences (Table 1) may provide supplementary information on the content of cystic lesions and in cases of hemorrhage (Fig. 6), and may offer possibilities for staging hemorrhage. As they are also flow-sensitive, moving fluids (e.g., in the pharynx) appear hyperintense.

10 Spectroscopy

In recent years, spectroscopy has been performed in the fetal setting, primarily to further assess the fetal brain (Kok et al. 2002; Heerschap et al. 2003; Girard et al. 2006a, b) (see Chap. 12), but also to study fetal lung maturation and its effects on the composition of amniotic fluid (Fenton et al. 2000; Clifton et al. 2006; Kim et al. 2008).

However, without fetal sedation, the long acquisition time (up to 5 min) may interfere with the successful acquisition of a spectrum. Nevertheless, readable spectra can be obtained in 73.3% of cases (Kulemann et al. 2009). In addition to fetal movements, the size and position of the voxel are important. Fetal brain spectroscopy may be complicated when there is little brain left, or when the fetus is in a breech presentation.

11 Three-Dimensional Dataset

Under ideal conditions, a continuous set of images devoid of fetal motion may be acquired, which is the prerequisite for volumetry and offers possibilities for reconstruction.

11.1 Volumetry

Volumetry of the fetus or fetal organs is being performed more often, especially to determine the size of the fetal

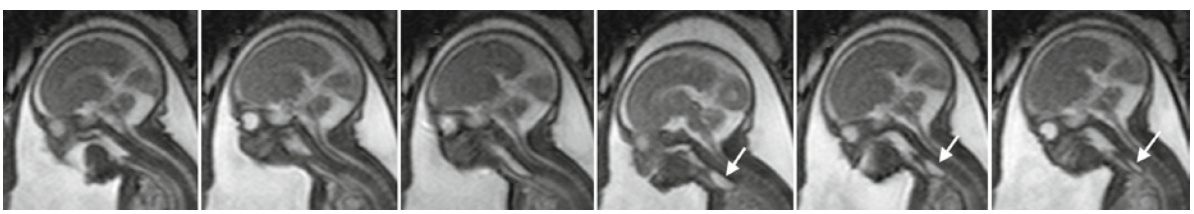

Fig. 13 Selected frames from a dynamic SSFP sequence that demonstrates swallowing in a fetus, with esophageal atresia, at 28+0 GW. The characteristic pouch sign (*arrow*) becomes apparent on the fourth image from the *left*

lungs in normal and pathological conditions (Kasprian et al. 2006; Ward et al. 2006) (see also Chap. 16). The region of interest is manually segmented on each slice, and its total area is multiplied by the distance between slices to compute the volume of an organ. Because of manual segmentation, volumetry is time-consuming. Depending on the size of the organ (lungs or liver), volumetry requires between 10 and 15 min; determining the total fetal body volume requires up to half an hour, depending on fetal size and the orientation of the stack, i.e., the number of slices (Cannie et al. 2006).

Since a continuous and nearly motion-free stack of images is essential for accurate volumetry, the sequence should be acquired during maternal breath-hold, especially when the fetus is vertically positioned. In that case, dislocation of the fetus along its vertical axis during acquisition of an axial stack may lead to images showing the same anatomy, or a cross section may be missed. This will lead to inaccuracies in volume determination. Therefore, the volumetry sequence should be checked for possible discontinuities that may affect volumetry. If this is the case, the sequence should be repeated.

The accuracy of volumetry will also depend on the size of the organ and on the section plane.

Choosing the plane with the least partial volume effects (e.g., axial for lungs) (Jani et al. 2005) will minimize this error. In general, it would appear that fetal MRI volumetry tends to overestimate organ volumes (lungs, liver) when compared to post-mortem organ volumetry (Jani et al. 2005).

11.2 Reconstruction

The acquisition of a continuous three-dimensional dataset covering the whole fetus would allow re-slicing of the stack of images in any desired section plane. However, the spatial resolution of such reformatted images is currently limited by the relatively large slice thickness, especially in smaller fetuses (Fig. 3). Recently, methods have been developed to produce self-consistent 3D volume images, even when motion occurs during the acquisition (Rousseau et al. 2006; Jiang 2008).

A motion-free dataset would also allow the creation of so-called three-dimensional reconstructions of the fetus (Fig. 14). However, this sort of reconstruction is rather time-consuming and the actual benefit remains to be determined.

12 Difficulties in Imaging

Difficulties in imaging an unsedated fetus usually result from fetal movements that complicate the acquisition of a continuous set of images, which are necessary to follow structures through the stack of images. Fortunately, constant fetal bulk movements throughout the study are infrequent.

It is commonly believed that, unlike ultrasound, MRI is not affected by maternal and fetal conditions, such as obesity and oligohydramnios. This calls for some

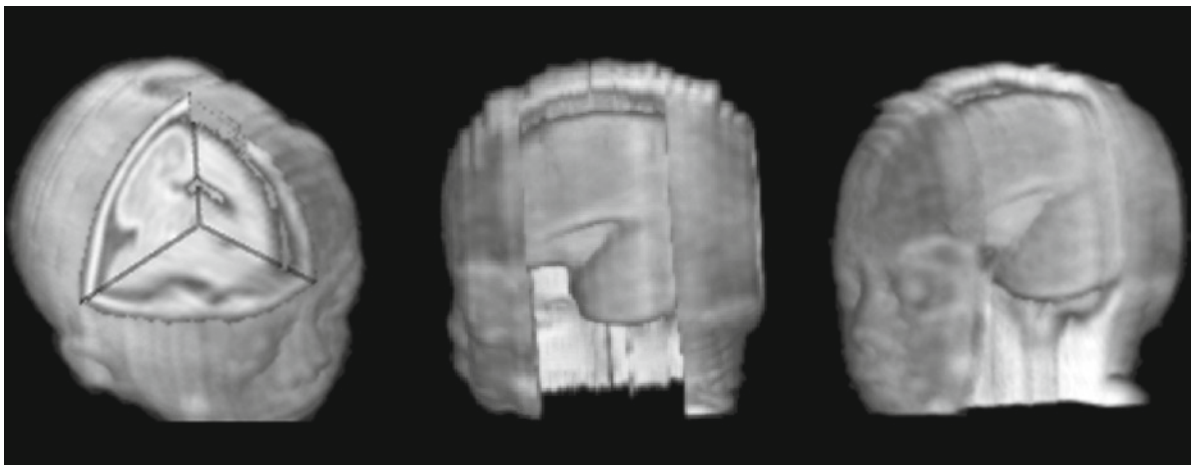

Fig. 14 Different views of a so-called "three-dimensional" reconstruction of the fetal head and brain at 24+2 GW, based on an inverted T2-weighted sequence acquired in the frontal plane. Note the irregular outline of the scalp due to manual segmentation in those areas where the head was in contact with the uterus

discussion, as these conditions can have an impact on image quality. Most notably, maternal overweight can pose problems for fetal MRI. While the table weight limit of 150 kg is less of a problem, the abdominal circumference in the supine position is more important, since it determines whether the pregnant woman fits into the bore of the magnet. While the gantry size differs between various types of magnets, in our experience, the upper limit of abdominal circumference in the supine position is about 135 cm. In such cases, the phased-array surface coil may not fit and the integral Q-body coil must be used, which leads to poorer image quality.

Abdominal circumference is also increased by marked polyhydramnios or multiple pregnancy. In polyhydramnios, apart from more space available for fetal movements, the fetus may be far away from the coil elements. In most cases, coil geometry can be improved by positioning the pregnant woman in the lateral decubitus position, which may bring the fetus closer to the coil elements.

By the end of pregnancy, pregnant women frequently do not tolerate the supine position well, and thus, have to be imaged in the lateral decubitus position. This, however, may be complicated or impossible when the pelvic width of the pregnant woman exceeds the height of the MRI gantry. When the fetal head requires examination, further problems may arise, since fetuses close to term usually have their head engaged within the lesser pelvis. This central position increases the distance of the fetal head from the fixed coil elements, which are now positioned at the maternal hip. Furthermore, placing the ventral coil elements above the pubic symphysis is difficult in the lateral decubitus position, because the thighs are flexed at the hip. This leads to an unfavorable coil geometry for imaging the fetal head. To complicate matters further, fetuses older than 34/35 GW, despite the little space available, tend to show pronounced head movements.

In fact, imaging multiple pregnancies is a challenge, especially when both fetuses need to be studied. Only rarely are the fetuses positioned, relative to each other, in such a way as to enable imaging of both in the same orthogonal plane. Moreover, movements of one fetus may be transferred to the co-twin. In feto-fetal transfusion syndrome, the acceptor presents with polyhydramnios and usually shows abundant movements, while the stuck twin, depending on its position within the uterus, may be subject to maternal breathing movements.

References

Baldoli C, Righini A, Parazzini C, Scotti G, Triulzi F (2002) Demonstration of acute ischemic lesions in the fetal brain by diffusion magnetic resonance imaging. Ann Neurol 52:243–246

Cannie M, Jani JC, De Keyzer F, Devlieger R, Van Schoubroeck D, Witters I, Marchal G, Dymarkowski S, Deprest JA (2006) Fetal body volume: use of MR imaging to quantify relative lung volume in fetuses suspected of having pulmonary hypoplasia. Radiology 241:847–853

Chaumoitre K, Colavolpe N, Shojai R, Sarran A, D' Ercole C, Panuel M (2007) Diffusion-weighted magnetic resonance imaging with apparent diffusion coefficient (ADC) determination in normal and pathological fetal kidneys. Ultrasound Obstet Gynecol 29:22–31

Clifton MS, Joe BN, Zektzer AS, Kurhanewicz J, Vigneron DB, Coakley FV, Nobuhara KK, Swanson MG (2006) Feasibility of magnetic resonance spectroscopy for evaluating fetal lung maturity. J Pediatr Surg 41:768–773

Ehrström C (1984) Circadian rhythm of fetal movements. Acta Obstet Gynecol Scand 63:539–541

Fenton BW, Lin CS, Ascher S, Macedonia C (2000) Magnetic resonance spectroscopy to detect lecithin in amniotic fluid and fetal lung. Obstet Gynecol 95:457–460

Girard N, Fogliarini C, Viola A, Confort-Gouny S, Fur YL, Viout P, Chapon F, Levrier O, Cozzone P (2006a) MRS of normal and impaired fetal brain development. Eur J Radiol 57:217–225

Girard N, Gouny SC, Viola A, Le Fur Y, Viout P, Chaumoitre K, D'Ercole C, Gire C, Figarella-Branger D, Cozzone PJ (2006b) Assessment of normal fetal brain maturation in utero by proton magnetic resonance spectroscopy. Magn Reson Med 56:768–775

Guimiot F, Garel C, Fallet-Bianco C, Menez F, Khung-Savatovsky S, Oury JF, Sebag G, Delezoide AL (2008) Contribution of diffusion-weighted imaging in the evaluation of diffuse white matter ischemic lesions in fetuses: correlations with fetopathologic findings. AJNR Am J Neuroradiol 29:110–115

Heerschap A, Kok RD, van den Berg PP (2003) Antenatal proton MR spectroscopy of the human brain in vivo. Childs Nerv Syst 19:418–421

Jani J, Breysem L, Maes F, Boulvain M, Roubliova X, Lewi L, Vaast P, Biard JM, Cannie M, Deprest J (2005) Accuracy of magnetic resonance imaging for measuring fetal sheep lungs and other organs. Ultrasound Obstet Gynecol 25:270–276

Jiang S (2008) Magnetic resonance imaging of the brain in moving subjects. Application to fetal, neonatal and adult brain studies. PhD Thesis, Imperial College London

Kasprian G, Balassy C, Brugger PC, Prayer D (2006) MRI of normal and pathological fetal lung development. Eur J Radiol 57:261–270

Kasprian G, Brugger PC, Weber M, Krssak M, Krampl E, Herold C, Prayer D (2008) In utero tractography of fetal white matter development. Neuroimage 43:213–224

Kim DH, Vahidi K, Caughey AB, Coakley FV, Vigneron DB, Kurhanewicz J, Mow B, Joe BN (2008) In vivo (1)H magnetic resonance spectroscopy of amniotic fluid and fetal lung at 1.5 T: technical challenges. J Magn Reson Imaging 28:1033–1038

Kim TH, Joh JH, Kim MY, Kim YM, Han KS (2002) Fetal pericallosal lipoma: US and MR findings. Korean J Radiol 3: 140–143

Kok RD, van den Berg PP, van den Bergh AJ, Nijland R, Heerschap A (2002) Maturation of the human fetal brain as observed by 1H MR spectroscopy. Magn Reson Med 48:611–616

Kulemann V, Brugger PC, Pugash D, Weber M, Prayer D (2009) Magnetic Resonance Spectroscopy of the fetal brain - does it work without sedation? ASNR 47th Annual Meeting 2009, Vancouver, Abstract book

Rousseau F, Glenn OA, Iordanova B, Rodriguez-Carranza C, Vigneron DB, Barkovich JA, Studholme C (2006) Registration-based approach for reconstruction of high-resolution in utero fetal MR brain images. Acad Radiol 13:1072–1081

Savelli S, Di Maurizio M, Perrone A, Tesei J, Francioso A, Angeletti M, La Barbera L, Ballesio L, de Felice C, Porfiri LM, Manganaro L (2007) MRI with diffusion-weighted imaging (DWI) and apparent diffusion coefficient (ADC) assessment in the evaluation of normal and abnormal fetal kidneys: preliminary experience. Prenat Diagn 27:1104–1111

Terakoshi H, Uchiyama K, Era K, Oishi S, Osone F, Futami T (2000) MR fetography. A new MR technique for imaging of the fetus. Jpn J of Magn Reson Med 20:138–149

Verswijvel G, Grieten M, Gyselaers W, Van Holsbeke C, Vandevenne J, Horvath M, Gelin G, Palmers Y (2002) MRI in the assessment of pregnancy-related intrauterine bleeding: a valuable adjunct to ultrasound? Jbr-Btr 85: 189–192

Ward VL, Nishino M, Hatabu H, Estroff JA, Barnewolt CE, Feldman HA, Levine D (2006) Fetal lung volume measurements: determination with MR imaging - effect of various factors. Radiology 240:187–193

Witzani L, Brugger PC, Hörmann M, Kasprian G, Csapone-Balassy C, Prayer D (2006) Normal renal development investigated with fetal MRI. Eur J Radiol 57:294–302